



UNIVERSITY OF LEEDS

This is a repository copy of *Tribological performance and tribochemical processes in a DLC/steel system when lubricated in a fully formulated oil and base oil*.

White Rose Research Online URL for this paper:

<http://eprints.whiterose.ac.uk/79921/>

Version: Accepted Version

Article:

Kosarieh, S, Morina, A, Laine, E et al. (2 more authors) (2013) Tribological performance and tribochemical processes in a DLC/steel system when lubricated in a fully formulated oil and base oil. *Surface and Coatings Technology*, 217. 1 - 12. ISSN 0257-8972

<https://doi.org/10.1016/j.surfcoat.2012.11.065>

Reuse

Unless indicated otherwise, fulltext items are protected by copyright with all rights reserved. The copyright exception in section 29 of the Copyright, Designs and Patents Act 1988 allows the making of a single copy solely for the purpose of non-commercial research or private study within the limits of fair dealing. The publisher or other rights-holder may allow further reproduction and re-use of this version - refer to the White Rose Research Online record for this item. Where records identify the publisher as the copyright holder, users can verify any specific terms of use on the publisher's website.

Takedown

If you consider content in White Rose Research Online to be in breach of UK law, please notify us by emailing eprints@whiterose.ac.uk including the URL of the record and the reason for the withdrawal request.

Tribological performance and tribochemical processes in a DLC/Steel system when lubricated in a fully formulated oil and base oil.

* Corresponding author. Tel.: +44 113 343 2119; fax: +44 113 242 4611. E-mail address: S.kosarieh10@leeds.ac.uk (S.Kosarieh).

S.Kosarieh^a,*, A. Morina^a, E.Lainé^b, J.Flemming^b, A.Neville^a

a Institute of Engineering Thermofluids, Surface and Interfaces (iETSI), School of Mechanical Engineering, University of Leeds, Leeds LS2 9JT, UK.

b Infineum UK Limited, 1 Milton Hill Abingdon, Oxfordshire, UK.

Abstract:

Diamond-like carbon (DLC) coatings show extremely good promise for a number of applications in automotive components as they exhibit excellent tribological properties such as low friction and good wear resistance. This can impact on improved fuel economy and durability of the engine components. Much work has been reported on the dry sliding of DLC coatings with less so in lubricated contacts and, as such, there is a need to further understand the tribochemistry of lubricated DLC contacts. Commercially-available oils are normally optimized to work on ferrous surfaces. Previous studies on DLC lubricated contacts have tended to use model oil systems rather than fully formulated lubricants and from this an interesting picture of lubrication mechanisms is emerging. Optimising compatibility between a surface and a set of lubricant additives may lead to excellent durability (wear) as well as increased fuel economy (low friction). In this work, the friction and wear properties of a DLC coating under boundary lubrication conditions have been investigated and the tribological performance compared with that of an uncoated steel system.

A pin-on-plate tribotester was used to run the experiments using High speed steel (HSS) M2 grade plates coated with 15 at.% hydrogenated DLC (a-C:15H) sliding against cast iron pins. A Group III mineral base oil, fully synthetic Group IV PAO and four different fully formulated oils were used in this study. Furthermore optical and scanning electron microscopes (SEM) were used to observe the wear scar and to

assess the durability of the coatings. Energy-Dispersive X-ray analysis (EDX), X-ray Photoelectron Spectroscopy (XPS) and Raman spectroscopy analyses were performed on the tribofilms to understand the tribochemical interactions between oil additives and the a-C:15H coating.

This study show that the durability of the a-C:15H coating strongly depends on the selected additive package in the oils. In addition the effect of detergent, dispersant and antioxidants on the performance of the Molybdenum-based friction modifier (Mo-FM) and ZDDP anti-wear additive were investigated and results are reported in this paper.

Keywords: DLC Coatings; Lubricant additives; ZDDP; Detergent; Dispersant; Antioxidant; MoDTC; Tribofilm; Boundary lubrication

1 Introduction

Increasing demand for improved fuel economy, ever-increasingly strict emission legislation and customer demand requires automotive companies to develop new strategies and apply them to two main areas; namely, materials and lubrication technology [1]. In recent years, reducing dependence on conventional P- and S-containing lubricant additives such as zinc dialkyldithiophosphate (ZDDP), which are harmful to catalytic converters and to the environment, has been one of the main concerns faced by lubricant industries. Applying new friction modifiers as well as implementing low friction and wear resistant coatings for engine components can potentially lead to reduction in the losses, improvement in fuel efficiency and to reducing dependence on P and S containing additives. Moreover, reducing the wear and frictional losses will extend the life time and improve the efficiency of the drive-line.

Diamond like carbon (DLC) is a carbon coating which has similar mechanical, optical, electrical and chemical properties to diamond but does not have the crystalline lattice structure; rather is an amorphous carbon coating having a network of sp^2 (graphite-like) and sp^3 (diamond-like) and hydrogen bonds. Diamond-like carbon is a term referred to a wide range of carbon base materials with excellent properties, like low coefficient of friction, high wear resistance, high hardness, chemical inertness, a relatively high optical gap, high electrical resistance and outstanding running-in properties [2, 3]. DLC may contain as high as 50 % hydrogen (a-C:15H) and as low as 1-2 % hydrogen (a-C) and it gives a coefficient of friction in the range of 0.1 to 0.02 when sliding against different metallic and ceramic counterparts in dry contacts. Several dopants, in the form of nano-particles such as metals are incorporated in the DLC coating matrix to reduce the internal stress as

well as enhancing the adhesion strength of the coatings [4, 5]. The properties of DLC depend significantly on the sp^2/sp^3 ratio as well as the hydrogen content, which in return, depends on the deposition process and applied parameters [6]. Robertson [5, 7] and Grill [8, 9] described the deposition methods to grow these films and to improve their mechanical properties. Offering excellent and outstanding tribological properties, DLC is being used extensively in the automotive industry as well as medical and other technical applications [6, 10].

At high temperatures of 300-400 °C, hydrogen in the a-C:15H coating starts to diffuse out of the coating matrix, giving rise to collapse of the sp^3 to a sp^2 structure, often referred to as “graphitisation” [11], and the transformation process completes at a high temperature of 700 °C or more [12]. The graphitisation of DLC plays an important role in friction reduction under dry sliding conditions [13-15]. Under tribological conditions, usually, the softer of the two materials will be worn while this is not the case for DLC. Wear products from DLC, which can have a graphite nature [16], can be transferred to the counter body forming a so-called transfer layer on the softer surface. The softer surface will then be protected from being worn off while the DLC slides over the transfer layer. The wear rate of DLC will also be extremely low after the transfer layer is formed. In addition the transfer layer also behaves as a solid lubricant [13, 17]. The formation and adhesion properties of this transfer layer depend strongly on the tribological and environmental conditions as well as the chemical properties of the counterpart [18].

Commonly-used friction modifiers and anti-wear additives are optimised to form tribofilms on ferrous surfaces. Molybdenum dithiocarbamate (MoDTC) and Zinc dialkyldithiophosphates (ZDDP) are well-known friction modifier and anti-wear additives respectively, used for ferrous surfaces. MoS₂ low friction sheets, derived

from MoDTC decomposition, provide low friction at the tribological contacts [19-21]. ZDDP offers anti-wear properties by forming sulphide and phosphate containing tribofilms at the ferrous surfaces [20-22]. In addition, MoDTC has been found to improve the wear resistance of the ferrous surfaces by forming N-containing species in the tribofilm [20]. With the emergence of new, non-ferrous coatings, researchers have started to consider how different lubricant additives interact with various types of DLC coatings under boundary lubrication. Podgornik et al. [23, 24] reported the chemical inertness of DLC coatings when lubricated in a commercially-available fully formulated oil. In addition, DLC coatings have been reported to be chemically inert using a steel pin sliding against DLC-coated disks lubricated in oil containing ZDDP and/or MoDTC [25]. In contrast, in recently published works, molybdenum-based friction modifiers have been reported to form low friction MoS₂ sheets and ZDDP-derived compounds were detected on the DLC coating providing low friction and better wear performance under boundary lubrication conditions [26-33]. Therefore, the published results have been found to be contradictory and a comprehensive understanding of DLC tribochemistry is still to be clearly produced.

The main objective of this work is to study the tribological performance of 15 at.% hydrogenated DLC coating (a-C:15H) under boundary lubrication conditions in presence of a Group III mineral base oil, fully synthetic Group IV PAO and four different fully formulated oils.

2 Experimental details

2.1 Pin-on-plate tests

Tests were performed using a reciprocating pin-on-plate tribometer under boundary lubrication conditions. The samples were cleaned prior to the start of the

test using acetone in an ultrasonic bath for 15 minutes. The contact point of the plate and pin was submerged under a static volume of lubricant (3 ml) at 100°C and the average linear speed was 20 mm/s (strike frequency of 1 Hz). A load of 390N was used that gave an initial Hertzian contact pressure of 0.7 GPa simulating a similar pressure range to a typical cam/follower contact gasoline engine. The friction force data was collected every **second** corresponding to two cycles and the duration of the tests was 6 hours. To evaluate friction performance, each type of test was repeated three times and average repeatability was seen to be less than 0.003 for the friction coefficient in the steady state region (i.e. last hour of the tests).

2.2 Materials

Tests were performed in the pin-on-plate tribotester using cast iron (CI) pins and coated/uncoated HSS M2 Grade steel plate. The dimensions of the CI pin were 20 mm in length, diameter 6 mm and the ends of the pins were machined with a 40 mm radius of curvature. The geometry of the flat plate was 15 mm×6 mm× 3mm. The physical properties of the coatings, substrate and pin are given in Table I.

The a-C:15H coating was deposited on the steel plate using a hybrid unbalanced magnetron sputter ion plating/PECVD deposition system and in all cases the substrates were cleaned by Ar⁺ plasma ion using pulsed DC bias prior to deposition of adhesion layer. In addition, a thin adhesion promoting Cr layer of approximately 0.2 µm thickness was deposited by DC magnetron sputtering with a pulsed DC bias followed by the introduction of nitrogen gas into the chamber. Then a CrC base layer was formed on the Cr layer by the addition of butane, controlled via a closed-loop optical emission monitoring system. Finally, a layer of a-C:15H was deposited using a pulsed DC bias on the substrate and a discharge enhancing electrode with a

13.56-MHz RF generator and the substrate temperature was maintained at less than 250°C for each coating run. The results of an uncoated (UC) steel/CI combination will also be presented in this study to compare the tribological performance of the a-C:15H /cast iron (CI) combination.

2.3 Lubricants

The lubricants used in this experiment are Group III mineral base oil, fully synthetic Group IV PAO and four different fully formulated oils. All the oils are supplied by Infineum UK limited and the key additive components in each oil are shown in Table II. Considering that the lubricants tested are commercial lubricants some chemical details are not possible to release. However the generic nature of anti-wear additives and friction modifiers which are keys to this study are described in detail.

Considering load, material and lubricant properties, the film thickness and lambda ratio were calculated using equations Eq 1 and Eq 2 respectively.

h_{min} , minimum film thickness, is numerically defined as [34, 35]:

$$\frac{h_{min}}{R'} = 3.63 \left(\frac{U\eta_0}{E'R'} \right)^{0.68} (\alpha E')^{0.49} \left(\frac{W}{E'^2} \right)^{-0.073} (1 - e^{-0.68k}) \quad \text{Eq 1}$$

Where η_0 is the dynamic viscosity at atmospheric pressure of the lubricant (4.03×10^{-3} Pas), α is viscosity-pressure coefficient (1.1×10^{-8} Pa⁻¹), R' is the reduced radius of curvature (20 mm), U is the entraining surface velocity (20 mm/s), W is the normal load (390 N), E' is the the reduced Young's modulus. The dynamic viscosity and viscosity-pressure coefficient were measured at 100°C.

$$\lambda = \frac{h_{min}}{\sqrt{R_{q1}^2 + R_{q2}^2}} \quad \text{Eq2}$$

Where R_{q_1} is the roughness of the coating and R_{q_2} is the roughness of the pin end.

The calculation gives the lambda ratio well under the unity (0.002) implying that the lubrication is in boundary regime.

2.4 Surface analysis

2.4.1 Pin Wear Measurements

Using fully formulated oils, the wear of the a-C:15H plates was not measurable and there was almost no variation in the roughness measurements. Therefore, wear coefficients are calculated from the wear diameter on the pin to indicate the lubricant effectiveness in wear reduction in the overall lubricating system. The wear scar diameters on the pins are calculated using the light microscope and then the volume of the lost segment of the sphere is calculated. Finally, the specific wear coefficients have been calculated using the Archard wear equation.

$$K_i = \frac{V_i}{F \times S} \quad \text{Eq3}$$

Where F is the normal load (N), S the sliding distance (m), V_i the wear volume (m^3), K_i and the dimensional wear coefficient and index i identifies the surface considered.

2.4.2 Coating wear analysis

In this study, a Zeiss EVO MA15 Variable Pressure SEM was used to investigate the mechanism of wear and the durability of the coatings. It was integrated with an Oxford Instruments Energy Dispersive X-ray (EDX) analysis system. In this study, the EDX analysis was used to provide information about the durability of the coating. EDX spectra obtained from inside the wear tracks showed presence of C and Cr inside the wear track. Cr comes from the underlying CrN/Cr intermediate layer and

so could be used as a semi quantitative measure of the coating thickness. The higher the Cr level, the lower the coating thickness (Figure 1). This method has been used before [36] and was shown to be effective in providing coatings wear performance.

Raman spectroscopy has been used as a technique to characterize DLC coatings, and their wear debris in the literature [37-39]. Renishaw inVia Raman microscope was used to analyze the structural modifications in the wear tracks of the a-C:15H coating and CI pin. The excitation wavelength used was 325.02 nm and the spectra were acquired with 10% power filter. The current intensity was controlled in order to achieve probing depth within 1 μm . The acquired Raman spectra usually comprised of distinct carbon peaks. In the Raman spectra recorded outside of the wear track, the G peak around 1580 cm^{-1} represents the graphite and D peak 1380 cm^{-1} represents the disorder-condensed benzene rings in amorphous carbon [38, 39]. The spectra were fitted with Lorenzian-Gaussian distributions associated with the peaks commonly found in amorphous hydrogenated carbon. In the actual analysis, the ratio of the intensity between the D and G peaks is considered to characterize the structure of the a-C:15H coating, rather than considering the overall intensity taken from one location to other. It is reported that the relative intensity height of the D peak is related to the microcrystalline size of the graphitic cluster, where less-graphitic amorphous films have a lower H_D/H_G value [40-43]. Therefore, higher values of the H_D/H_G ratio imply transformation of the a-C:15H coating into graphite in the a-C:15H matrix under the present boundary-lubricated conditions [39].

2.4.3 Chemical analysis of the tribofilms

XPS analysis was carried out for the chemical analysis of the tribofilm formed on the plate surfaces. XPS was performed

This sensitive technique can probe as small as a few nanometers (5 nm) depth in the surface. The samples were cleaned using n-heptane to remove residual oil and contaminants before doing XPS analysis. The spot size was 500 μm with a power of 150W and all the measurements were performed using a VG Escalab 250 XPS with monochromated aluminium K-alpha X-ray source. Spatial mode was chosen to acquire the spectra. CasaXPS software [44] was used to fit the curves on XPS peaks obtained from long scans and the quantitative analyses of the peaks were performed using peak area sensitivity factors. A handbook of XPS [45] has been used to find the chemical species at the respective binding energies. The position of C1s peak (284.8 eV) was considered as the reference for charge correction to obtain information with the most appropriate chemical meaning, the peak area ratio, difference between binding energies of the doublets, and full-width at half-maximum (FWHM) were constrained. The data presented in this study have been processed, taking into account a linear background approximation. A standard set of sensitivity factors held within the data analysis software was used. The quantification results were mainly given in a comparative mode between different tribofilms, making use of these factors acceptable.

3 Results

3.1 Friction Results

The friction coefficient as a function of time for the a-C:15H/Cl combination using five different oils is given in Figure 2. Based on the friction traces, it can be seen that all the fully formulated oils followed the same trend with time. The average friction coefficient values for the last hour of the test as a function of lubricants for a-C:15H/Cl system versus steel/Cl system are given in Figure 3. Overall, friction

performance of all the oils are different for the steel/CI compared to the a-C:15H/CI system and the friction coefficients were observed to be oil dependant. The friction coefficients in the a-C:15H/CI system were generally lower than for the steel/CI system except for the cases where the MoDTC type friction modifier (Mo-FM) was blended in combination with other additives in the oil. As expected in the steel/CI system, the addition of ZDDP to the fully formulated oils (Oil1+ and Oil2+) gave rise to an increase in friction in comparison to the non-ZDDP containing oils (Oil1- and Oil2-). The same response was also observed in the a-C:15H/CI system for Oil1+ (in comparison to Oil1-). Conversely, the presence of Mo-FM in the Oil2+ formulation in combination with ZDDP gave a small reduction in friction in comparison to the ZDDP free version of this oil (Oil2-).

It is interesting to note that a drop in friction was observed when PAO and Base oil (group III) with no additives were used. Additive-free PAO showed a drop in friction 2hrs after the start of the tests providing the lowest steady state coefficient of friction of all the oils in the a-C:15H/CI system. In Figure 4, it is shown how wear products from a-C:15H are transferred to the counter body forming a transfer layer on the pin. The transfer materials are accumulating around the edges of the wear scars on the pins.

In order to investigate the possible effect of the transfer layer formed on friction reduction, the pin and the plate were cleaned by acetone every hour during the test to assure that no transfer material resided on the interface. The aim was to observe any deviation in terms of friction and wear of the pin. In Figure 5 the friction response after the transfer material was removed every hour during the test is shown. It can be seen that removing the transfer layer during the test hindered friction reduction.

3.2 Coating durability and wear results

The wear provided the fully formulated oils on both a-C:15H/Cl and steel/Cl systems was observed to be very low making the wear measurements of the plates extremely difficult.

Figure 6 shows representative images of the wear scar; it is evident that the extent and mechanisms of wear is dependent on the additive package used in the lubricant. Severe delamination of the a-C:15H coating at multiple regions was seen when lubricated in PAO (Figure 6a) while Group III base oil (Figure 6b) gave mild delamination on the a-C:15H coated plate. In contrast in fully formulated oils (Figure 6c-f) there was no delamination; rather, the wear of the coatings was dominated by gradual polishing wear. It should be mentioned that, in this study, the terminology delamination refers to removal of the coating from the substrate. For coatings lubricated with the ZDDP-containing oil there was virtually no wear as reported elsewhere [36]. Friction modifier containing fully formulated oils (Oil2+ and Oil2-) were also observed to have almost no wear. Oil1+ and Oil1- provided microscratches on the wear scar of the coating. The colour of the wear tracks was brighter than outside of the wear track suggesting exposure of the underlying Cr/CrN layers, as a result of the loss of coatings. Oil1+ (ZDDP-containing fully formulated oil) showed more coating removal than Oil1- (ZDDP-free Oil1+) confirming the ineffectiveness of ZDDP in wear protection when combined with detergent, dispersant and antioxidants thus is in agreement with wear measurements which will be discussed later and are shown in Figure 9 . In addition, SEM analysis was carried out in the wear scars of the a-C:15H coated plate to investigate coating durability (Figure 7). Observations from SEM images showed good agreement with the optical microscope images and wear results.

To verify the observations from SEM results and optical microscope images, EDX was carried out in the wear scar. It is important to note that, the SEM/EDX analysis in this study was performed to check the durability of coating, not to characterize tribofilms. Therefore tribofilm on the plates were removed using acetone prior to the SEM/EDX analysis.

EDX spectra obtained from inside the wear tracks showed presence of C and Cr inside the wear track. The difference between concentration of Cr in the wear tracks and outside of the wear tracks was used to identify the wear performance of various oils which are shown in Figure 8. The repeatability of the results for the coating durability was considered obtaining spectra in three different places across the wear tracks for tests using the same oil. Analysing PAO was impractical due to the fact that PAO showed severe delamination on the a-C:15H-coated sample plate.

Based on the results, it is apparent that fully formulated oils showed very little difference in concentration of Cr implying very low gradual wear on the coated plates which is in agreement with the initial observation when trying to measure the wear on the plates. Highest gradual wear was observed for additive-free base oil Group III.

The wear coefficients of the CI counterbodies for various oils are given in Figure 9. Regardless of the tribological system, Oil1+ and Oil2+ oils showed higher wear compared to Oil1- and Oil2- oils. This suggests that ZDDP is less effective in wear protection of the counterbody when was used together with detergent, dispersant and antioxidant. PAO showed lower pin wear than fully formulated oils in the a-C:15H/CI system while providing the highest wear in the steel/CI system.

As discussed earlier, in order to investigate the possible effect of formed transfer layer on the wear protection of the counter body, the pin and the plate were cleaned by acetone during the test. Shown in Figure 10, it can be seen that removing the

formed transfer layer during the test not only hindered friction reduction but increased the pin wear.

3.3 Chemical Analysis of Tribofilms

The chemical analysis of the tribofilms was performed using XPS on the wear scars of the plates. The binding energies of the main fitted peaks and corresponding chemical species for a-C:15H/Cl and Steel/Cl system are shown in Table III and Table IV, respectively. It is evident that the amount of Mo 3d detected on the tribofilm in fully formulated oils is insignificant for both a-C:15H/Cl and steel/Cl systems. In addition, regardless of the tribo-system, a P peak was detected on all the ZDDP containing fully formulated oils in the a-C:15H/Cl system (Figure 11).

Zn 2p peaks were also found on both a-C:15H/Cl and steel/Cl system for all the ZDDP containing oils. The binding energies of the ZDDP-derived elements suggest that, all fully formulated oils formed ZnS/ZnO/Zn-phosphate on both systems. Phosphate was also found in the tribofilm formed from Oil2+ (ZDDP-containing fully formulated oils in combination with Mo-FM) in both a-C:15H/Cl and steel/Cl systems. In the a-C:15H/Cl system, Fe 2p peak was not detected in the tribofilms using any of the oils suggesting that the coating was not delaminated and that the iron coming from the pin worn particles did not take part in the tribofilm formation on the a-C:15H surface.

In this study, PAO provided the lowest friction and highest wear on the a-C:15H plate and based on the physical observation transfer layer was not formed on the pins using all fully formulated oils. Therefore, Raman spectroscopy analysis was only performed in the wear scars of the a-C:15H coating and Cl pin when PAO was used. This technique was done to understand the structural modifications of a-C:15H

within the wear track and the nature of wear debris transferred to the CI counterbody from the worn a-C:15H coating.

Figure 12 shows Raman spectra obtained using PAO from (a) outside of a-C:15 coating wear scar, (b) inside of a-C:15H coating wear scar, (c) transfer material on the pin and (d) out of wear scar of pin. As shown in Figure 12, the value of the ratio H_D/H_G and the full-width at half-maximum (FWHM) of the G peak show slight difference within and outside the wear scar of the a-C:15H coating suggesting that no structural modification of the a-C:15H coating due to the tribological test in the wear scar have happened. Interestingly, distinct G and D peaks were observed in the wear scar on the CI pin, and no such peak was observed outside the wear scar. The H_D/H_G ratio for the transfer material on the CI pin was found to be higher than a-C:15H coating and FWHM of the G peak decreased, which indicates that the transfer of the material to the CI pin was more of graphitic nature material.

Furthermore, the D and G peaks were not found in the spectrum taken from outside the wear scar of the CI pin suggesting that the graphite flakes, which are normally present in the microstructure of the cast iron, did not participate in formation of the transfer layer on the pins. In fact, the graphite present in the microstructure of CI was apparently not enough to give a distinct G peak compared with the coating material.

4 Discussion

4.1 Effect of oil chemistry on coating delamination

Having a graphite-like structure through transferring worn materials from the a-C:15H coating to the interface could significantly reduce friction in dry conditions [13-15]. Graphitisation could be initiated by high temperature (400 °C) causing the

hydrogen to be diffused out of the a-C:15H matrix which in return results in collapse of the random covalent structure of a-C:15H and provide a graphitic layer. Based on a simple model, asperity temperature rise due to friction (friction-induced temperature) can be calculated by Eq 4 [13, 46].

$$\Delta T = \frac{1}{4} \frac{\mu Pv}{(K_{DLC} + K_{CI})a} \quad \text{Eq 4}$$

where $a = (\frac{P}{\pi H})^{\frac{1}{2}}$, ΔT is the induced temperature rise, μ the friction coefficient, P is the applied normal load, v the sliding speed, K_{DLC} and K_{CI} are the thermal conductivities of the a-C:15H coating and CI counterbody, respectively, a the contact radius of the real contact area, and H is the measured hardness of the a-C:15H coating.

Considering the highest obtained coefficient of friction and the experimental parameters of this study, the rise of the temperature at the contact was not significant (20°C). Therefore, the friction-induced temperature was too low to be responsible for the phase transformation of the a-C:15H coating.

The phase transformation temperature of DLC coating is a function of contact pressure which can be expressed by Eq 5 [47].

$$T = T_c \exp \left[\frac{\Delta v}{L} \Delta p \right] \quad \text{Eq 5}$$

Where T_c is the critical phase transformation temperature ($= \sim 350^{\circ}\text{C}$), L is the phase transition energy of diamond ($15.6 \times 10^4 \text{ J kg}^{-1}$), Δv is the difference between the specific volume of hydrogen-free ($0.284 \times 10^{-3} \text{ m}^3 \text{ kg}^{-1}$) and hydrogenated coating ($0.294 \times 10^{-3} \text{ m}^3 \text{ kg}^{-1}$ to $0.416 \times 10^{-3} \text{ m}^3 \text{ kg}^{-1}$), Δp is the difference between Hertzian contact pressure and atmospheric pressure.

Using Eq 5 and taking into account the experimental parameters of this study, the phase transformation temperature of a-C:15H coating is much higher than the operating temperature of the experiments (100°C). Therefore, the Hertzian contact pressure exerted by the counterbody on the a-C:15H coating was not likely to be responsible for the graphitisation. However, according to Clapeyron law (Eq 5) transformation of a-C:15H could occur at a much lower temperature when subjected to high pressure (stressed-induced graphitisation) [14]. Generation of ferrous wear particles from the worn CI counterbody along with the scratches with positive edges on the surface, decrease the contact area and increase the contact pressure significantly. Thus, subsequently reduces the temperature required for initiation of graphitisation and accelerate the graphitisation process [48, 49]. Estimation of the phase transformation temperature for DLC coating has also been reported elsewhere [39, 50] showing the important role of contact pressure on structural changes of a-C:15H.

Additive-free PAO used in this study provided comparatively lower friction while showing severe delamination of the a-C:15H surface as well as high gradual wear. The high contact pressure exerted by positive edges of the scratches [48] and “micro-size” iron particles coming from the counterbody [50] could be responsible for graphitisation of the a-C:15H surface which consequently could lead to severe delamination of the a-C:15H coating. It is interesting that the pin wear provided by PAO was less than those of fully formulated oils. It could be argued that wear products from a-C:15H, which have a graphite nature (Figure 12), are transferred to the counter body forming a transfer layer on the pin in the first two 2hrs of the tests (Figure 4). The pin surface will then be protected from being worn off while the a-C:15H slides over the transfer layer. It should be noted that transfer layer has low

shear strength and is progressively removed from the surface [14]. Increasing graphitisation and removal and transfer of materials to the counterbody with time will lead to gradual thinning of the a-C:15H coating which in return will decrease the load bearing capability of the a-C:15H coating. With the poor load bearing capability of the coating, the high shear stress is transmitted to the substrate causing plastic deformation to the substrate/intermediate layer which leads to debonding of the Cr interlayer form the substrate and to the coating failure accordingly [51].

A similar low friction and high gradual abrasive/polishing wear was observed when base oil group III was used but mild delamination was seen after 6hrs of the tests. Nevertheless both base oils showed higher wear of the a-C:15H coating and lower friction compared to fully formulated oils. On the other hand the pin wear in the a-C:15H/CI system using base oil group III was higher than all other oils. Considering mild delamination/graphitization on the coating and the fact that there was no additive blended in the base oil to form any possible protective tribofilm on the pin surface, it can be argued that less transfer materials have been transferred to the pin surface and thus resulted in less wear protection.

Additives in fully formulated oils could suppress graphitization by providing a “tribochemical protective layer” on the interface. Additive-derived anti-wear compounds could inhibit the formation of wear particles which in return could avoid pressure induced graphitization. The ability of additives to suppress graphitization was also reported by Kalin et al. [52]. The formed tribofilm could also prevent the counterbody from excessive wear which could explain why less wear was observed on the pins when additized oils were used compared to the base oil in the a-C:15H/CI system.

4.2 Tribochemistry of a-C:15H

4.2.1 Effect of oil additives interaction on tribofilm formation

Fully formulated oils contain different additives including detergent and dispersant. They are blended in a fully formulated engine oil to form a film on the part surface preventing deposition of sludge and varnish and to keep oil insoluble contaminants and degradation products in suspension, at elevated temperature for detergents and at low temperatures for the dispersant additives. However, interaction between different additives when used together in formulated oils could result either in synergistic or antagonistic effects modifying the characteristics of the protective surface tribofilms which in return affects the oil performance regarding anti-wear and frictional responses [53].

Shown in Figure 13, it is evident that using fully formulated oils, detergent and dispersant-derived elements were detected on both steel and a-C:15H surface. However, the nature of Ca and N species formed on a-C:15H were different from those of steel ones but their mode of action in which they could affect tribofilm formation on the surface is still unclear and is a matter of further study. Nevertheless, the presence of Ca and N on the surface could have an effect on formation of FM-derived tribofilms on both a-C:15H and steel surfaces resulting in comparatively high friction values observed from fully formulated oils.

4.2.2 Anti-wear film formation

The obtained results clearly showed the critical role of selected additives in the oils on the durability of the coating which is in agreement with previous findings [36, 50]. Zn-phosphate and ZnS/ZnO species were formed in the tribofilms using all the fully formulated oils and the presence of Mo-FM in the oil did not affect phosphate film

formation on the surface for Oil2+ and Oil1+ oils. It could be probably due to the low concentration of Mo-FM in the fully formulated Oil2+ oil.

As mentioned earlier, ZDDP in combination with Mo-FM showed friction reduction in the a-C:15H/CI system seen when comparing Oil2- with Oil2+. In the steel/CI system, ZDDP increased friction when added to the lubricant which is in agreement with the literature where formation of pad-like tribofilm was identified as the reason for such higher friction [54].

4.3 Lubrication comparison of a-C:15H/CI and steel/CI

Based on this study, friction and wear results obtained from steel/CI system were generally different from those of a-C:15H/CI system. ZDDP usually decomposes on the ferrous surfaces and then it reacts with Fe_2O_3 from either wear debris/ ferrous surface and form strongly bonded Zn-phosphate anti-wear compounds [55-57]. Comparing the XPS atomic concentration of ZDDP-derived elements formed on the surface, it can be seen that the amount of Zn and P elements are higher on steel surface than a-C:15H. This suggests that a thicker film is obtained when the surface was ferrous.

Comparing the pin wear results, a-C:15H greatly reduces the wear of the counterbody when additive-free base oils were used. The formed transfer layer on the pins could protect the pin surface from further wear providing a lower wear on the pins which in return it will results in higher wear on the plate. In addition the transfer layer could also behave as a solid lubricant justifying the low friction provided by the base oils in the a-C:15H/CI system which is discussed in detail earlier. In contrast, all fully formulated oils showed higher wear of the pins in the a-C:15H/CI system. It can be explained by the fact that using fully formulated oils, the wear rate on the a-C:15H

plates was extremely low, the friction reduction was not observed and based on the physical observations(Figure 4); transfer layer is not formed on the pins. Thus, as mentioned earlier, under tribological conditions, usually, the softer of the two materials which in this study is cast iron will be worn.

5 Conclusions

The following conclusions can be drawn from this study:

- ZDDP decomposed under boundary lubrication condition and formed Zn-phosphate/ZnS/ZnO anti-wear species in the tribofilms formed on a-C:15H. In contrast, the amount of Mo 3p detected on the a-C:15H surface was very low using fully formulated oils.
- a-C:15H coating durability is strongly oil dependant and the coating failure can be avoided using additive containing oils which form a protective tribofilm on the surfaces and suppress the a-C:15H coating structural modification. Base oil group III performed better wear performance than PAO suggesting the important role of selection of base oil in the lubricant.
- Fully formulated oils demonstrated a good wear performance of the a-C:15H coatings. FM containing fully formulated oils showed almost no wear while the main wear mechanisms on the FM free fully formulated oils were polishing.
- Friction reduction is not significant using fully formulated oils mainly due to the phosphate formed on the surface. In addition presence of detergent, dispersant, antioxidant could affect Mo-FM-derived film formation.

Acknowledgment

Authors would like to express their deepest appreciation to the University of Leeds and Infineum UK Ltd. for funding this project and to Dr. Toby Middlemiss of Oerlikon Balzers Coating UK Ltd. for supplying the coatings.

References

1. Enomoto, Y. and T. Yamamoto, *New materials in automotive tribology*. Tribology Letters, 1998. **5**(1): p. 13-24.
2. Kodali, P., K.C. Walter, and M. Nastasi, *Investigation of mechanical and tribological properties of amorphous diamond-like carbon coatings*. Tribology International, 1997. **30**(8): p. 591-598.
3. Ronkainen, H., S. Varjus, and K. Holmberg, *Friction and wear properties in dry, water- and oil-lubricated DLC against alumina and DLC against steel contacts*. Wear, 1998. **222**(2): p. 120-128.
4. Ronkainen, H., J. Likonen, and J. Koskinen, *Tribological properties of hard carbon films produced by the pulsed vacuum arc discharge method*. Surface and Coatings Technology, 1992. **54-55**(Part 2): p. 570-575.
5. Robertson, J., *Diamond-like amorphous carbon*. Materials Science and Engineering: R: Reports, 2002. **37**(4-6): p. 129-281.
6. Hauert, R., *An overview on the tribological behavior of diamond-like carbon in technical and medical applications*. Tribology International, 2004. **37**(11-12): p. 991-1003.
7. Robertson, J., *Hard amorphous (diamond-like) carbons*. Progress in Solid State Chemistry, 1991. **21**(4): p. 199-333.
8. Grill, A., *Tribology of diamondlike carbon and related materials: an updated review*. Surface and Coatings Technology, 1997. **94-95**: p. 507-513.
9. Grill, A., *Diamond-like carbon: state of the art*. Diamond and Related Materials, 1999. **8**(2-5): p. 428-434.
10. Platon, F., P. Fournier, and S. Rouxel, *Tribological behaviour of DLC coatings compared to different materials used in hip joint prostheses*. Wear, 2001. **250**(1-12): p. 227-236.
11. Tallant, D.R., et al., *The thermal stability of diamond-like carbon*. Diamond and Related Materials, 1995. **4**(3): p. 191-199.
12. Ong, C.W., et al., *Thermal stability of pulsed laser deposited diamond-like carbon films*. Thin Solid Films, 1995. **258**(1-2): p. 34-39.
13. Liu, Y., A. Erdemir, and E.I. Meletis, *A study of the wear mechanism of diamond-like carbon films*. Surface and Coatings Technology, 1996. **82**(1-2): p. 48-56.

14. Voevodin, A.A., et al., *Friction induced phase transformation of pulsed laser deposited diamond-like carbon*. Diamond and Related Materials, 1996. **5**(11): p. 1264-1269.
15. Sánchez-López, J.C., et al., *Friction-induced structural transformations of diamondlike carbon coatings under various atmospheres*. Surface and Coatings Technology, 2003. **163-164**: p. 444-450.
16. Gütler, J. and J. Reschke, *Metal-carbon layers for industrial application in the automotive industry*. Surface and Coatings Technology, 1993. **60**(1-3): p. 531-535.
17. Hirvonen, J.-P., et al., *Tribological characteristics of diamond-like films deposited with an arc-discharge method*. Journal of Materials Research, 1990. **5**(11): p. 2524-2530.
18. Liu, Y., A. Erdemir, and E.I. Meletis, *Influence of environmental parameters on the frictional behavior of DLC coatings*. Surface and Coatings Technology, 1997. **94-95**: p. 463-468.
19. Grossiord, C., et al., *MoS₂ single sheet lubrication by molybdenum dithiocarbamate*. Tribology International, 1998. **31**(12): p. 737-743.
20. Morina, A., et al., *ZDDP and MoDTC interactions and their effect on tribological performance – tribofilm characteristics and its evolution*. Tribology Letters, 2006. **24**(3): p. 243-256.
21. De Barros, M.I., et al., *Friction reduction by metal sulfides in boundary lubrication studied by XPS and XANES analyses*. Wear, 2003. **254**(9): p. 863-870.
22. Martin, J.-M., et al., *Transfer films and friction under boundary lubrication*. Wear, 2000. **245**(1-2): p. 107-115.
23. Podgornik, B., S. Jacobson, and S. Hogmark, *Influence of EP additive concentration on the tribological behaviour of DLC-coated steel surfaces*. Surface and Coatings Technology, 2005. **191**(2-3): p. 357-366.
24. Podgornik, B., S. Jacobson, and S. Hogmark, *DLC coating of boundary lubricated components--advantages of coating one of the contact surfaces rather than both or none*. Tribology International, 2003. **36**(11): p. 843-849.
25. Kano, M., Y. Yasuda, and J.P. Ye, *The effect of ZDDP and MoDTC additives in engine oil on the friction properties of DLC-coated and steel cam followers*. Lubrication Science, 2004. **17**(1): p. 95-103.
26. de Barros'Bouchet, M.I., et al., *Boundary lubrication mechanisms of carbon coatings by MoDTC and ZDDP additives*. Tribology International, 2005. **38**(3): p. 257-264.

27. Haque, T., et al., *Non-ferrous coating/lubricant interactions in tribological contacts: Assessment of tribofilms*. Tribology International, 2007. **40**(10-12): p. 1603-1612.
28. Miyake, S., et al., *Improvement of boundary lubrication properties of diamond-like carbon (DLC) films due to metal addition*. Tribology International, 2004. **37**(9): p. 751-761.
29. Haque, T., et al., *Study of the ZDDP Antiwear Tribofilm Formed on the DLC Coating Using AFM and XPS Techniques*. J. ASTM Int. Journal of ASTM International, 2007. **4**(7).
30. de Barros'Bouchet, M.I., et al., *Improved mixed and boundary lubrication with glycerol-diamond technology*. Tribology - Materials, Surfaces & Interfaces, 2005. **1**: p. 28-32.
31. Haque, T., A. Morina, and A. Neville, *Influence of friction modifier and antiwear additives on the tribological performance of a non-hydrogenated DLC coating*. Surface and Coatings Technology, 2010. **204**(24): p. 4001-4011.
32. Vengudusamy, B., et al., *Tribological properties of tribofilms formed from ZDDP in DLC/DLC and DLC/steel contacts*. Tribology International, 2011. **44**(2): p. 165-174.
33. Vengudusamy, B., et al., *Behaviour of MoDTC in DLC/DLC and DLC/Steel contacts*. Tribology International, 2012. **54**(0): p. 68-76.
34. Hamrock, B.J. and D. Dowson, *Ball bearing lubrication : the elastohydrodynamics of elliptical contacts*. 1981, New York: Wiley.
35. Stachowiak, G.W. and A.W. Batchelor, *Elastohydrodynamic Lubrication*, in *Engineering Tribology (Third Edition)*. 2006, Butterworth-Heinemann: Burlington. p. 287-362.
36. Haque, T., A. Morina, and A. Neville, *Effect of Friction Modifiers and Antiwear Additives on the Tribological Performance of a Hydrogenated DLC Coating*. Journal of Tribology-Transactions of the Asme. **132**(3): p. 13.
37. Zhang, H.S. and K. Komvopoulos, *Direct-current cathodic vacuum arc system with magnetic-field mechanism for plasma stabilization*. Review of Scientific Instruments, 2008. **79**(7): p. 073905-7.
38. Schwan, J., et al., *Raman spectroscopy on amorphous carbon films*. Journal of Applied Physics, 1996. **80**(1): p. 440-447.
39. Zhou, Z.F., et al., *Study of tribological performance of ECR-CVD diamond-like carbon coatings on steel substrates: Part 2. The analysis of wear mechanism*. Wear, 2005. **258**(10): p. 1589-1599.

40. Prawer, S., et al., *Systematic variation of the Raman spectra of DLC films as a function of sp₂:sp₃ composition*. Diamond and Related Materials, 1996. **5**(3–5): p. 433-438.
41. Ferrari, A.C. and J. Robertson, *Interpretation of Raman spectra of disordered and amorphous carbon*. Physical Review B, 2000. **61**(20): p. 14095-14107.
42. Tay, B.K., et al., *Raman studies of tetrahedral amorphous carbon films deposited by filtered cathodic vacuum arc*. Surface and Coatings Technology, 1998. **105**(1–2): p. 155-158.
43. Scheibe, H.J., D. Drescher, and P. Alers, *Raman characterization of amorphous carbon films*. Fresenius' Journal of Analytical Chemistry, 1995. **353**(5): p. 695-697.
44. Fairley, N., *CasaXPS version 2.3.15*. Casa Software Ltd.
45. Moulder, J.F., et al., *Handbook of x-ray photoelectron spectroscopy. A reference book of standard spectra for identification and interpretation of xpsdata*. 1992, Eden Prairie, MN: Physical Electronics.
46. Rabinowicz, E., *Friction and wear of materials*. 1965, New York: Wiley.
47. Le Huu, T., et al., *Transformation of sp₃ to sp₂ sites of diamond like carbon coatings during friction in vacuum and under water vapour environment*. Thin Solid Films, 1996. **290-291**: p. 126-130.
48. Jaoul, C., et al., *Raman analysis of DLC coated engine components with complex shape: Understanding wear mechanisms*. Thin Solid Films, 2009. **518**(5): p. 1475-1479.
49. Abdollah, M.F.B., et al., *Phase transformation studies on the a-C coating under repetitive impacts*. Surface and Coatings Technology. **205**(2): p. 625-631.
50. Haque, T., et al., *Effect of oil additives on the durability of hydrogenated DLC coating under boundary lubrication conditions*. Wear, 2009. **266**(1-2): p. 147-157.
51. Villiger, P., C. Sprecher, and J.A. Peters, *Parameter optimisation of Ti-DLC coatings using statistically based methods*. Surface and Coatings Technology, 1999. **116-119**: p. 585-590.
52. Kalin, M. and J. Vizintin, *Real contact temperatures as the criteria for the reactivity of diamond-like-carbon coatings with oil additives*. Thin Solid Films, 2010. **518**(8): p. 2029-2036.
53. Bec, S., et al., *Synergistic Effects of MoDTC and ZDTP on Frictional Behaviour of Tribofilms at the Nanometer Scale*. Tribology Letters, 2004. **17**(4): p. 797-809.

54. Spikes, H., *The History and Mechanisms of ZDDP*. Tribology Letters, 2004. **17**(3): p. 469-489.
55. Martin, J.M., et al., *Synergistic effects in binary systems of lubricant additives: a chemical hardness approach*. Tribology Letters, 2000. **8**(4): p. 193-201.
56. Aktary, M., M.T. McDermott, and J. Torkelson, *Morphological evolution of films formed from thermooxidative decomposition of ZDDP*. Wear, 2001. **247**(2): p. 172-179.
57. Piddock, A.J. and G.C. Smith, *Scanning probe microscopy of automotive anti-wear films*. Wear, 1997. **212**(2): p. 254-264.

Table I Physical properties of plates (substrate/coatings) and counterpart materials

Properties of coating and other related materials	Ferrous Material		DLC Coating
Specification	HSS M2 Grade	Cast iron BS1452	a-C:15H ^a
Hardness	8.0 GPa	4.0 – 4.5 GPa	17.0 GPa
Reduced Young's modulus	218 GPa	134 GPa	190 GPa
Roughness, R_q	0.04-0.06 μm	0.07-0.09 μm	0.04-0.06 μm
Composition/ Coating thickness	C 0.64%, Si 0.55%, Cr 1.57%, and Mn 0.49%	C 3.0%, Si 2.0%, Mn 0.4%, Cr 0.1%, Cu 0.3%	<0.5 CrC <0.5 Cr 2-3 μm

^a Commercial coatings obtained from Oerlikon Balzers Ltd., UK.

Table II Lubricant components

Lubricants	Annotations	Base stock	Additives
PAO	PAO	Group IV	N/A
Base oil	Base oil	Group III	N/A
Fully formulated oil without FM	Oil1+	Group III	ZDDP Detergent Dispersant Antioxidant
Fully formulated oil with FM	Oil2+	Group III	ZDDP MoDTC-type friction modifier (Mo-FM) OFM- Organic friction modifier Detergent Dispersant Antioxidant
Fully formulated oil without FM and ZDDP	Oil1-	Group III	Detergent Dispersant Antioxidant
Fully formulated oil with FM but without ZDDP	Oil2-	Group III	MoDTC-type friction modifier (Mo-FM) OFM- Organic friction modifier Detergent Dispersant Antioxidant

Table III binding energies, concentration of XPS and corresponding chemical in the tribofilms formed on a-C:15H coated plates by oils Oil1+, Oil2+ and Oil2-.

Oils	Binding Energies, chemical species and concentrations			
	S 2p peaks	Mo 3d peaks	P 2p peaks	Zn 2p peaks
a-C:15H coated plates				
Oil1+	-	-	133.7 eV, metaphosphate (100%)	1022.5 eV, ZnS/ZnO/Zn-phosphate (100%)
Oil2+	163.6 eV, sulphide (68.7 %) 168.4 eV, sulphate (15.2 %) 171.1 eV, sulphate (16.1 %)	Small to fit the curve	133.8 eV, metaphosphate (100%)	1022.6 eV, ZnS/ZnO/Zn-phosphate (95%) 1024.4 eV, ZnS/ZnO (5%)
Oil2-	163.6 eV, sulphide (34.1%) 168.1 eV, sulphate (49.9%) 169.8 eV, sulphate (16.0%)	Small to fit the curve	-	-

Table IV binding energies, concentration of XPS and corresponding chemical in the tribofilms formed on steel coated plates by oils Oil1+, Oil2+ and Oil2-.

Oils	Binding Energies, chemical species and concentrations			
	S 2p peaks	Mo 3d peaks	P 2p peaks	Zn 2p peaks
Steel plates				
Oil1+	-	-	133.1 eV, pyrophosphate (100%)	1022.0 eV, ZnS/ZnO/Zn- phosphate (100%)
Oil2+	160.8 eV, sulphide (75.0 %) 167.5 eV, sulphate (25.0 %)	Small to fit the curve	132.8 eV, pyrophosphate (100%)	1021.5 eV, ZnO/Zn- phosphate (100%)
Oil2-	160.1 eV, sulphide (10.9 %) 167.0 eV, sulphate (59.3%) 168.9 eV, sulphate (29.8%)	229.2 eV, MoS ₂ (17.2%) 230.8 eV M (v) (31.8%) 232.6 eV Mo-oxide (15.3%) 226.6 eV, S 2s (35.5%)	-	-

Table of figures

Figure 1 Schematic diagram showing the cross section of the a-C:15H coating plate.

Concentration of Cr, detected by EDX, is higher inside the wear track compared to outside.

Figure 2. Friction traces as a function of time for the a-C:15H/CI system for oils Base, Oil1+, Oil2+, Oil1- and Oil2-.

Figure 3. Steady state friction coefficients as a function of lubricants for a-C:15H/CI system versus Steel/CI system.

Figure 4 Transfer layer on the pin coming from the wear track of a-C:H coating when (a) PAO, (b) Base oil group III, (c) Oil1+, (d) Oil2+, (e) Oil1- and (f) Oil2- were used.

Figure 5 Friction response after cleaning transfer material every hour during the test.

Figure 6 Optical images of the wear scars formed on the a-C:15H coated plates using (a) PAO, (b) Base oil Group III, (c) Oil1+, (d) Oil2+, (e) Oil1- and (f) Oil2-.The arrows on the left side of the images show sliding directions.

Figure 7 SEM images of the wear scars formed on the a-C:15H coated plates using (a) PAO, (b) Base oil Group III, (c) Oil1+, (d) Oil2+, (e) Oil1- and (f) Oil2-.The arrows on the left side of the images show sliding directions.

Figure 8 Difference between concentrations of Cr inside the wear tracks and outside of the wear tracks using various oils.

Figure 9. Dimensional wear coefficients as a function of lubricants for a-C:15H/CI systems...

Figure 10 Effect of cleaning transfer layer on friction and wear.

Figure 11 P2p curve fitting for ZDDP containing fully formulated oils on a-C:15H plates.....

Figure 12 Raman spectroscopic analysis on the samples obtained using PAO. Hd and Hg are the intensity height of D and G peaks, respectively. The colored boxes on the optical image of the CI pin and the SEM image of a-C:15H coating show the sites where the Raman analyses were carried out.....

Figure 13 Detergent-derived Ca peak (a) and dispersant-derived N peak (b) using fully

formulated oils.....

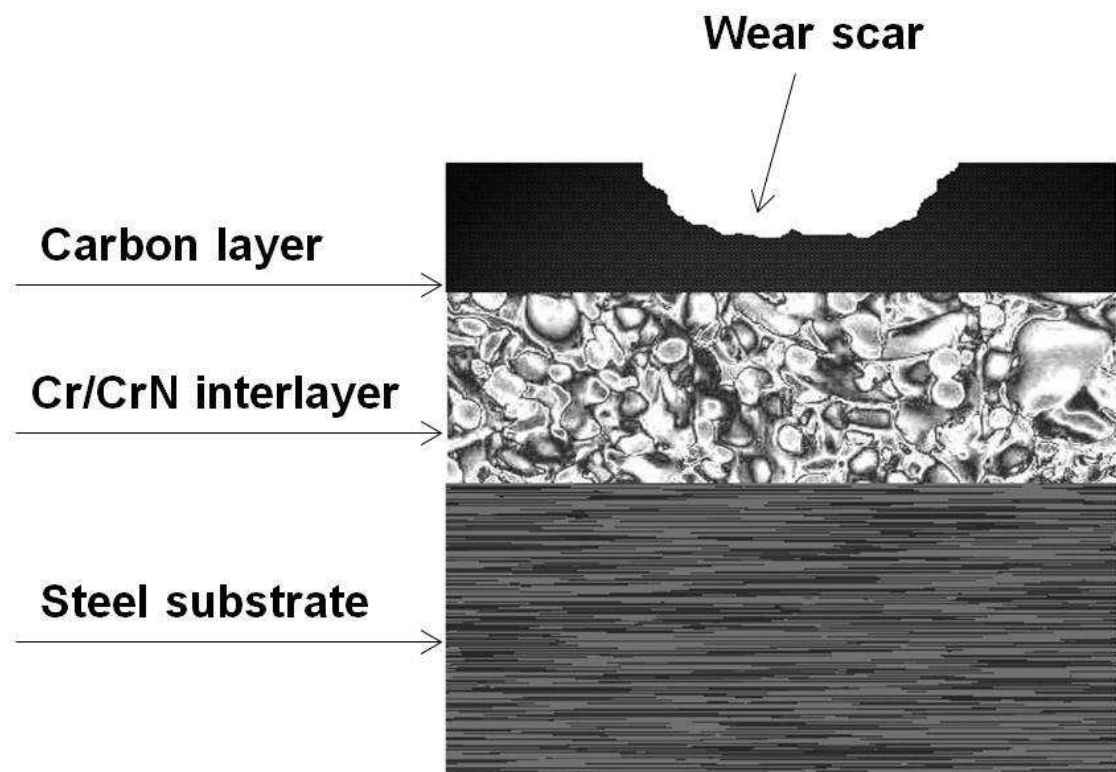


Figure 1

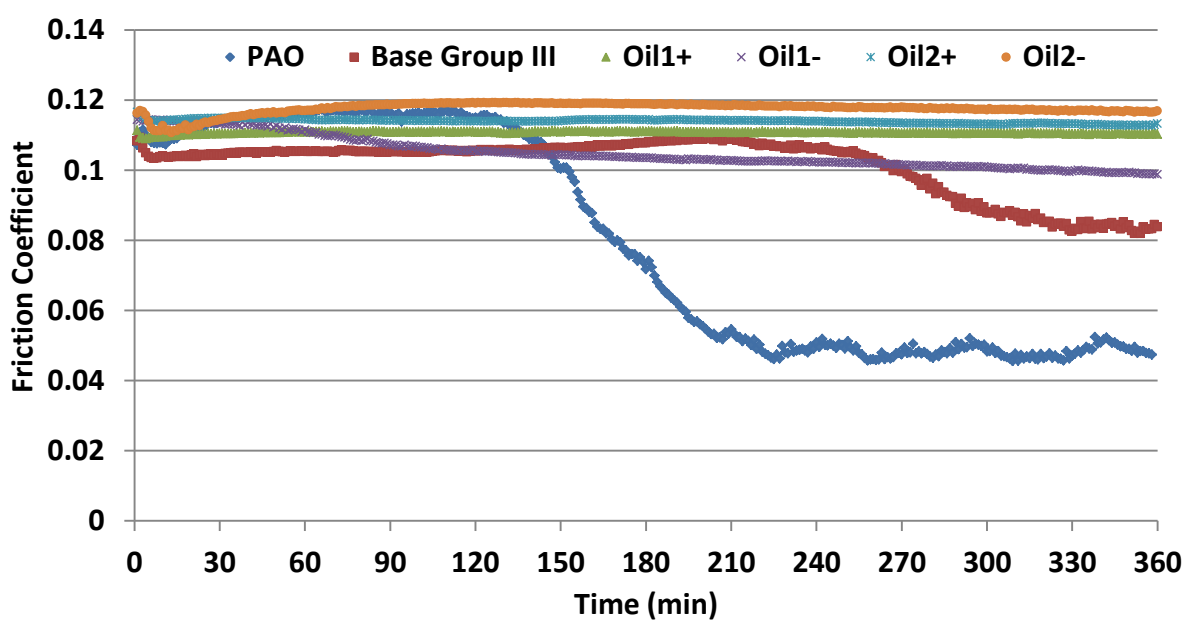


Figure 2

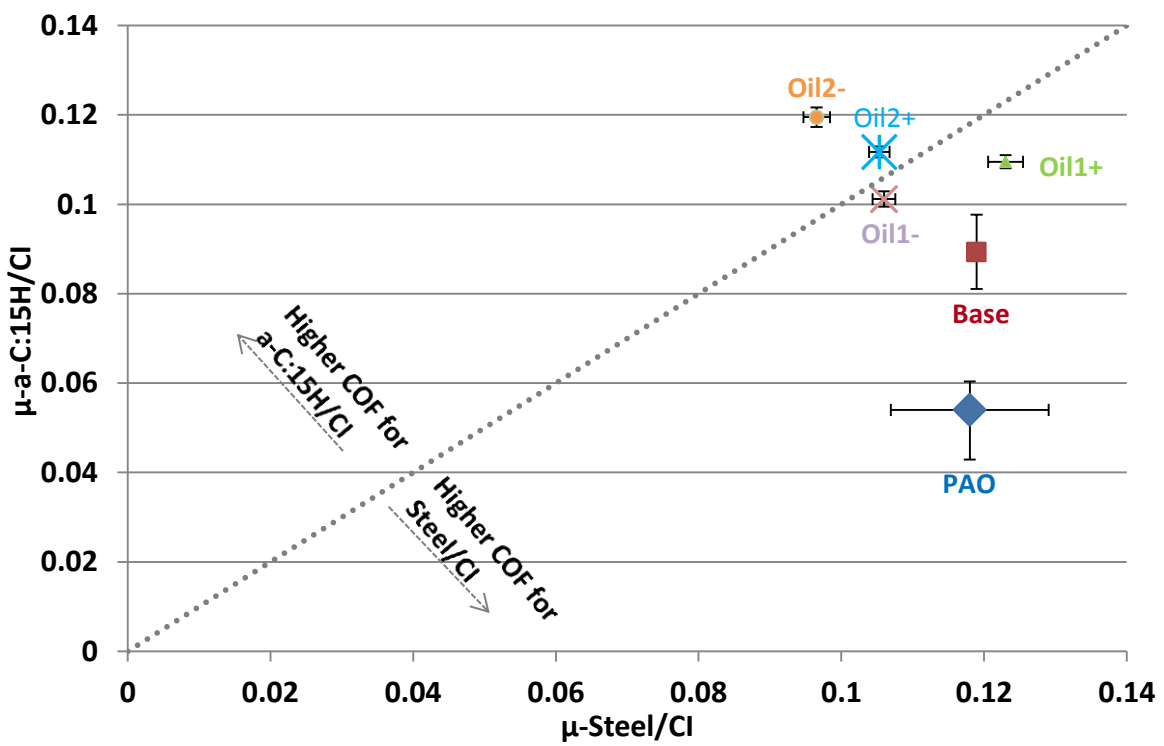


Figure 3

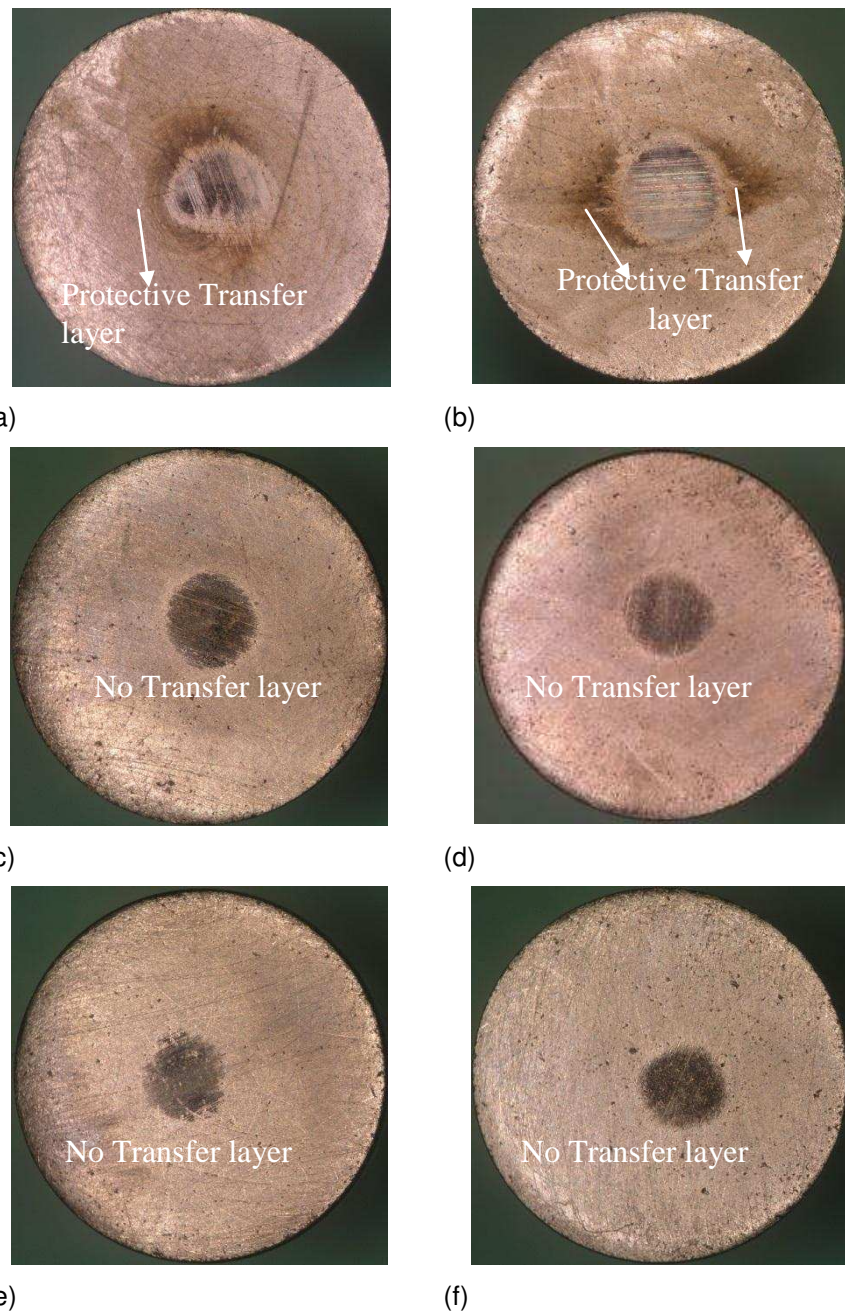


Figure 4

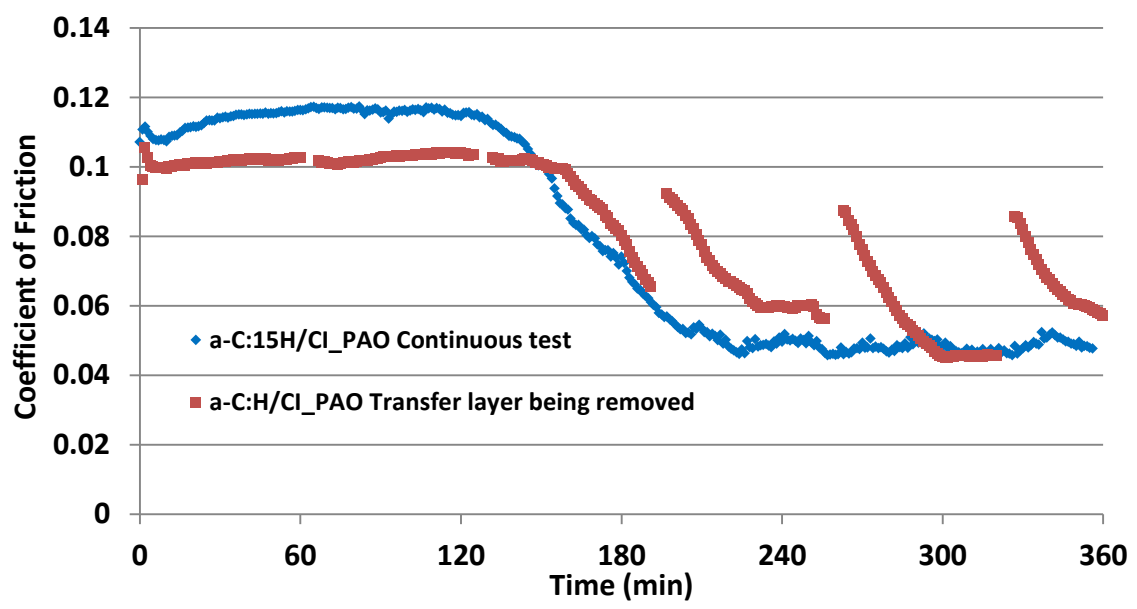


Figure 5

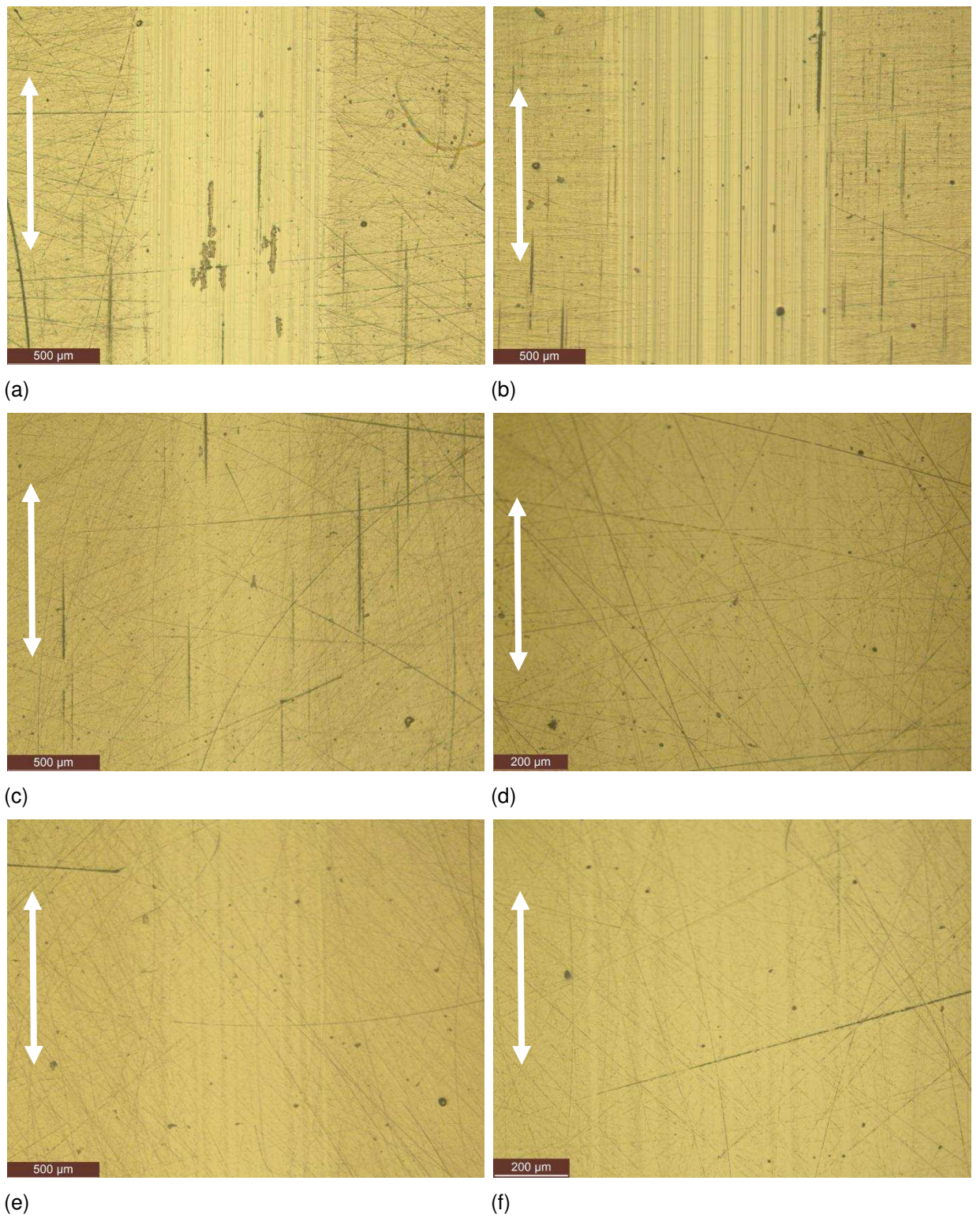


Figure 6

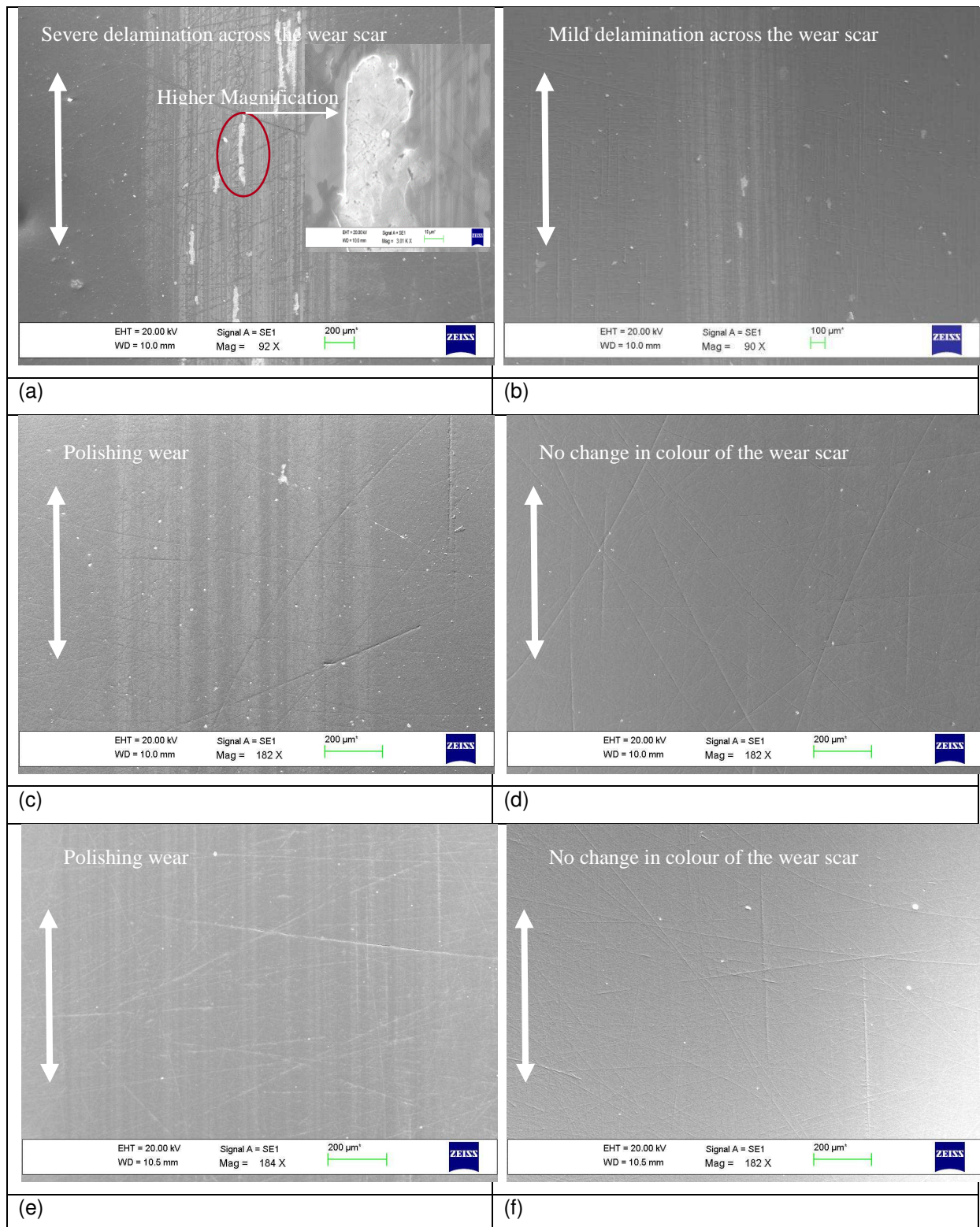


Figure 7

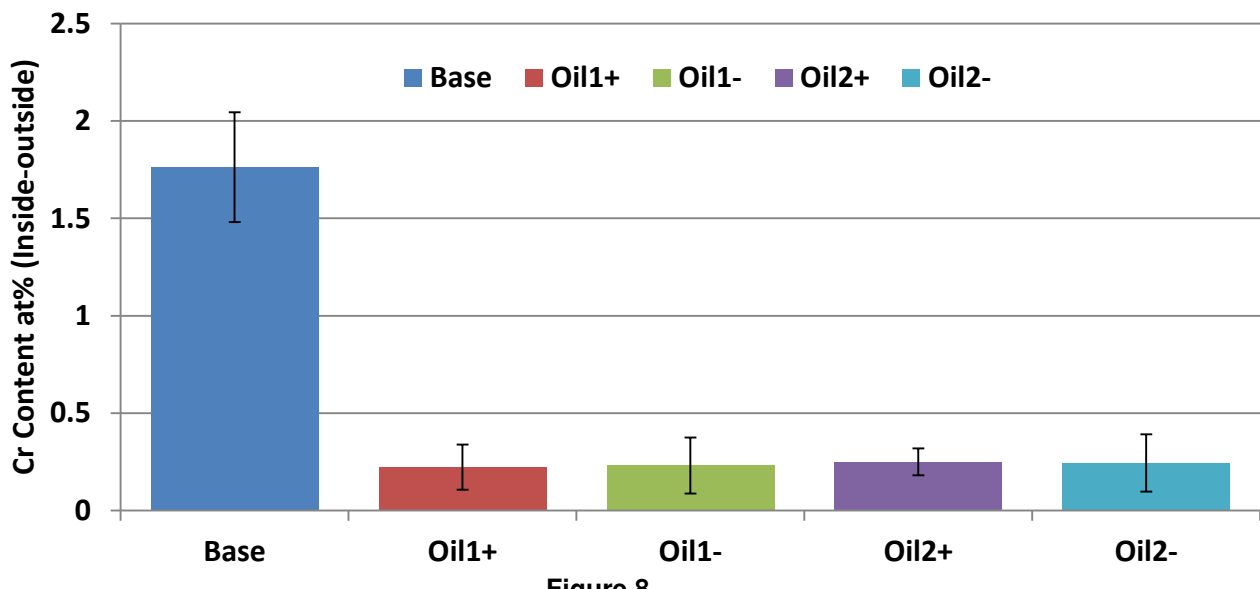


Figure 8

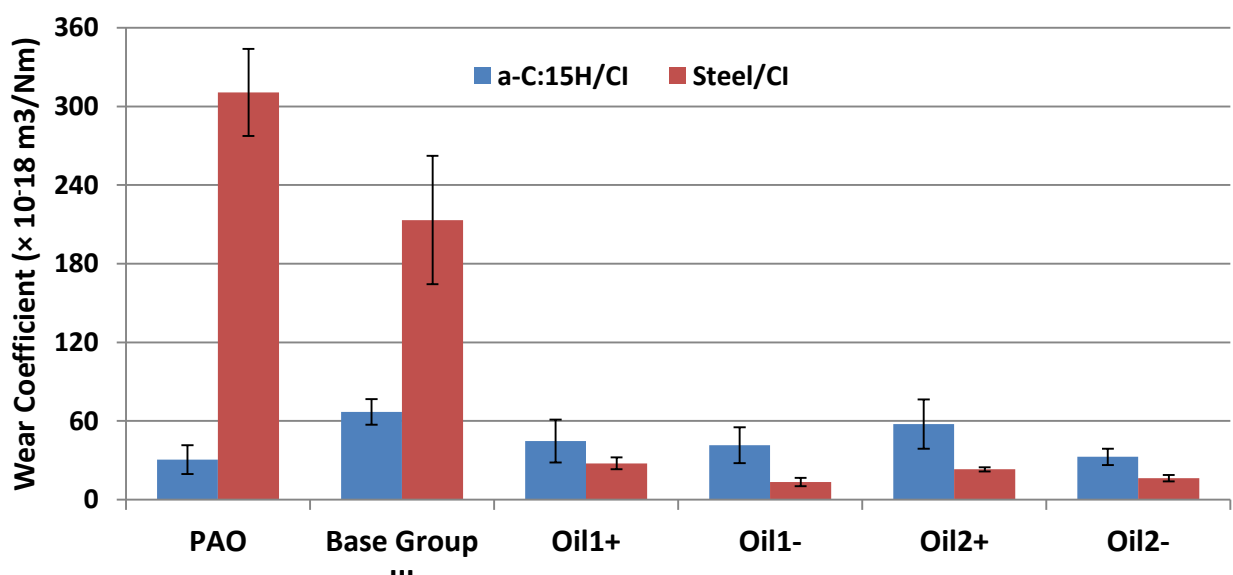


Figure 9

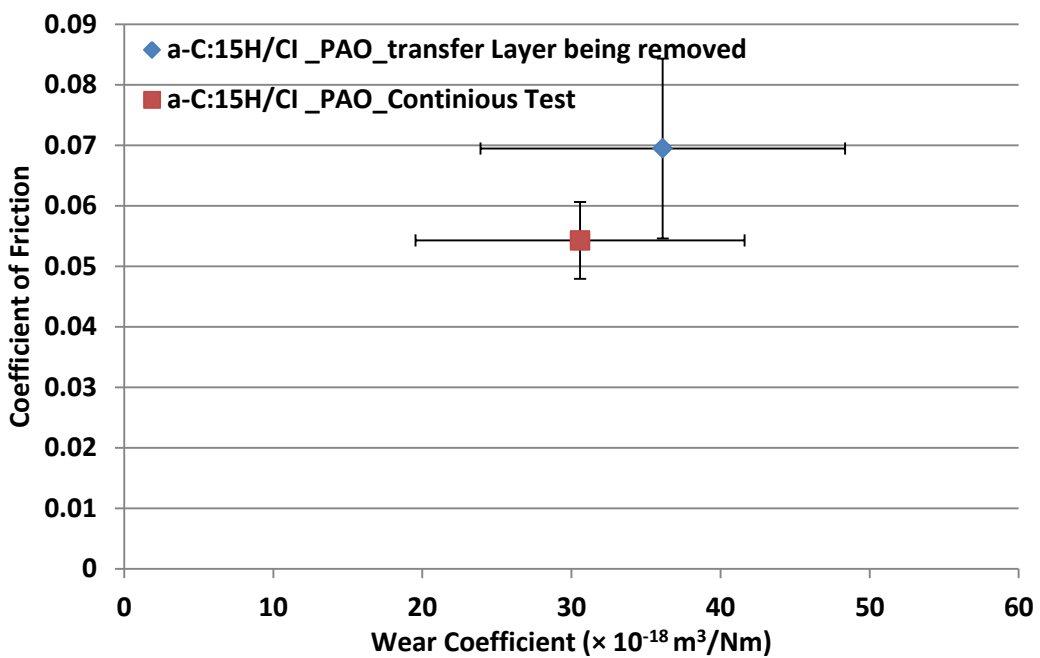


Figure 10

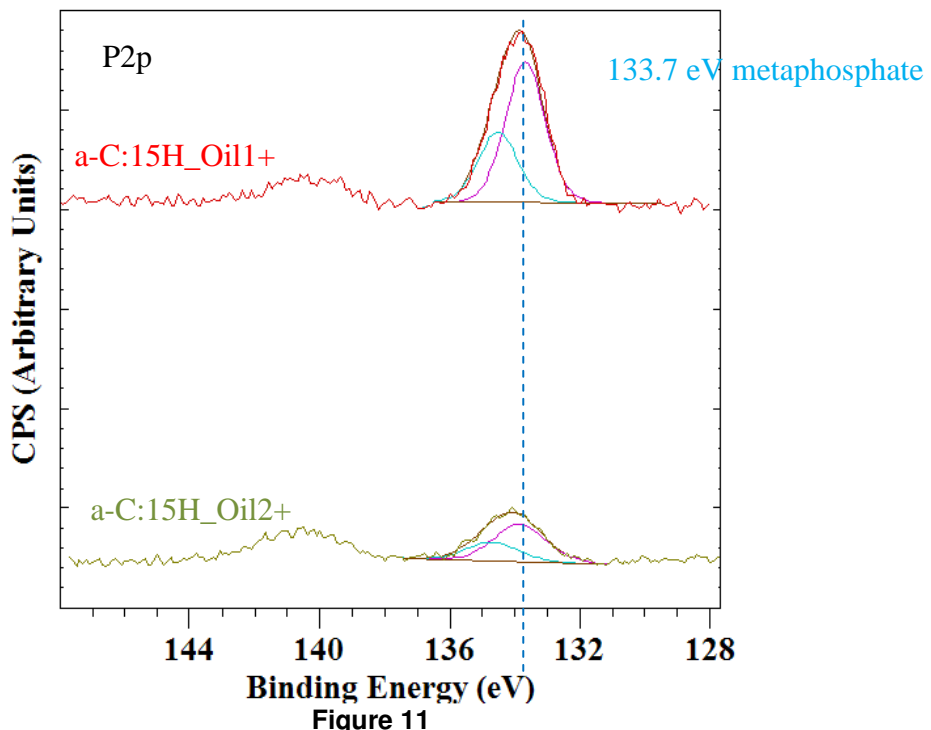


Figure 11

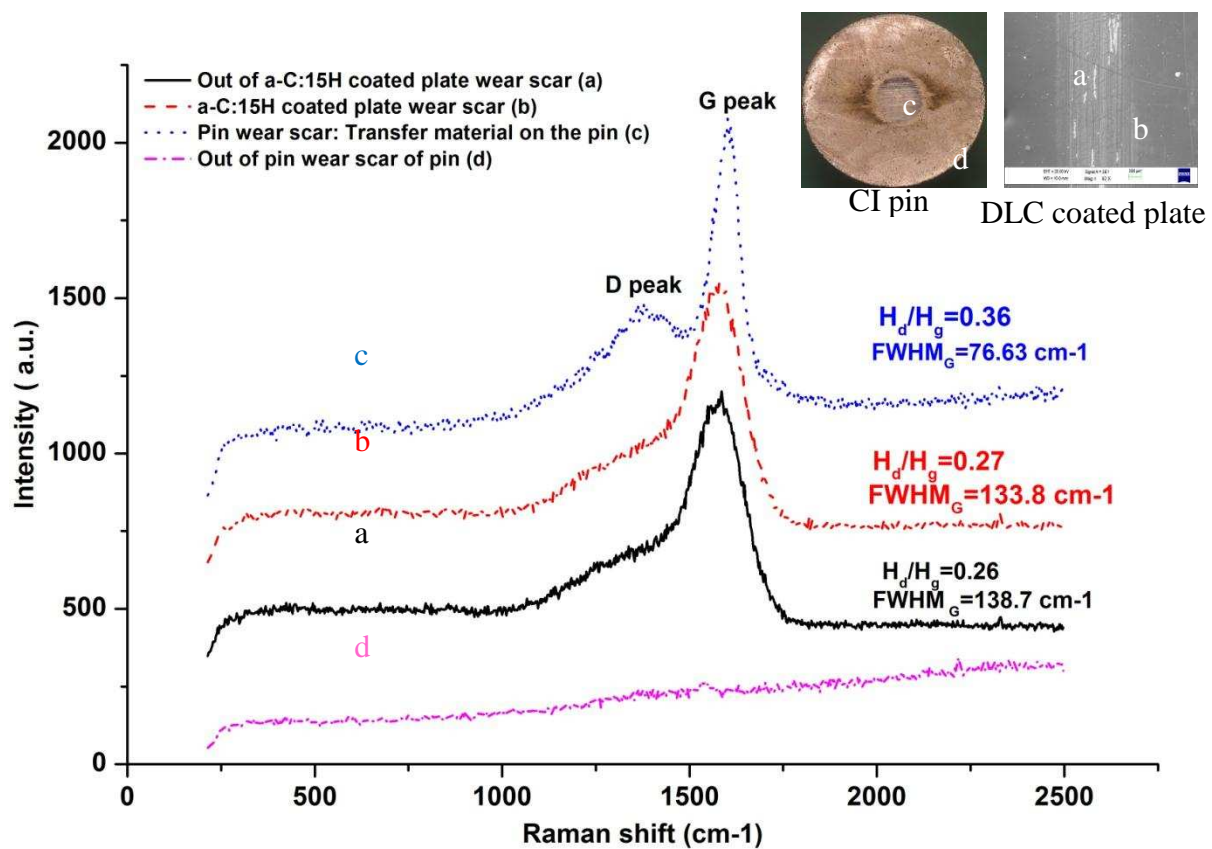
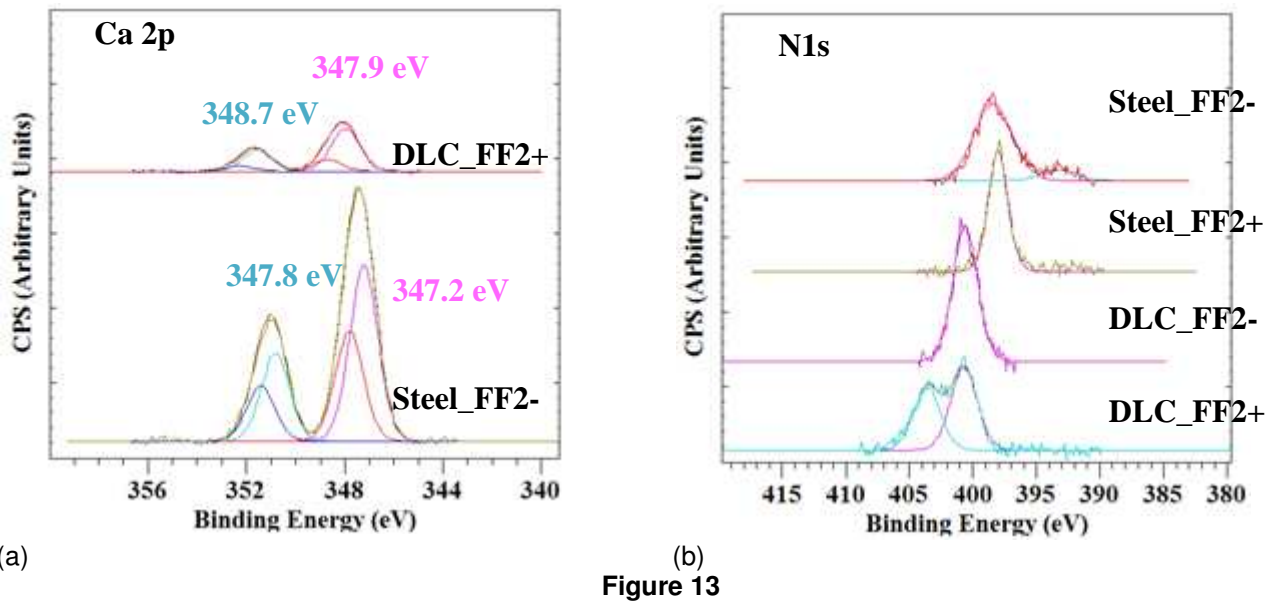


Figure 12



(b)
Figure 13